mathematics

MDPI

Review

Memristor Cellular Nonlinear Networks

Angela Slavova [1,*] and Ventsislav Ignatov [2]

[1] Institute of Mathematics and Informatics, Bulgarian Academy of Sciences, 1113 Sofia, Bulgaria
[2] Laboratory of Engineering Mathematics, Ruse University "Angel Kanchev", 7017 Ruse, Bulgaria; vignatov@uni-ru.bg
* Correspondence: slavova@math.bas.bg

Abstract: This paper presents a review of the theory and applications of memristor cellular nonlinear networks. By mapping the physical processes to the memristive framework, all resistive switching devices can be modeled. The idea is to find a state variable that presents with high accuracy the important features of the system, its dynamics, and time evolution in response to the inputs of the memristor. In order to develop a new design of memristor-based cellular nonlinear networks (MCNN), new circuital and mathematical memristor models need to be introduced. In this way, implementation into new software packages for computer-aided integrated circuit realization can be achieved. Another challenging problem is studying the complex behavior of MCNN models by means of local activity theory and generalizing it for various test cases. An application of the hardware implementation of these models can be found in nanostructures.

Keywords: memristor; cellular nonlinear networks; memristor cellular nonlinear networks; pattern formation

MSC: 92B20; 92C15; 35B36; 68T10

Citation: Slavova, A.; Ignatov, V. Memristor Cellular Nonlinear Networks. *Mathematics* **2023**, *11*, 1601. https://doi.org/10.3390/math11071601

Academic Editors: Pedro A. Castillo Valdivieso, Andrea Scozzari and Zhao Kang

Received: 25 January 2023
Revised: 27 February 2023
Accepted: 23 March 2023
Published: 26 March 2023

1. Introduction

Classical computers have the unique property to be algorithmically programmable, which was invented by J. von Neumann and which means they use mainly binary logic and arithmetic on discrete valued data (binary codes). It is known that the Turing machine is based on the mathematical concept of a universal machine in which the neurons work as threshold logic, using the main structure of the brain. In 1948, transistors were invented, as well as integrated circuits in 1960, and this made computer architecture a very practical, cheap and ubiquitous commodity. Soon after that, however, it was discovered that the neurons operate in a different way. Since, at this time, the electronic industry was developed using a huge number of transistors, a nanoscale size and many pixels, new characteristics of modern computers appeared [1]: parallel processors using the two-dimensional structure of silicon and optical technology; two-dimensional cellular structures together with a sub-100 nm size, giving power dissipation and wire length constraints; millions of analog sensory signals, which were organized in arrays and embedded in sensory computing devices; image flows, such as multi-spectral visual and tactile, becoming typical data; bionic array interfaces appearing, which made possible the mimicking of complex living organisms, such as muscle or retina prostheses; spatiotemporal devices, which made it possible to produce high complexity in time and space; software systems with high-performance grids and mobile communications with standardized interfaces. Nowadays, we find many dynamically programmable tiny sensor processors arranged in fixed arrays or on ad hoc platforms. For this reason, a new architecture is needed to develop spatiotemporal control and processing software. The invention of cellular nonlinear networks (CNN) [1] makes all this possible.

CNN consist of cells [1] that are connected to each other within small neighborhoods. This is the algorithm for the construction of the programmable cellular dynamics of CNN by elementary instruction:

(a) we take a dynamical system; let us call it a cell (with input u, state x and output y);
(b) we place the cells into the spatial grid with their neighborhood relations;
(c) we process the spatial interactions between the dynamic cells, being programmable (called the cloning template or gene, or simply the template);
(d) we add cellular sensors for the application of CNN in image processing.

In this review, we shall present the theory and applications of memristor cellular nonlinear networks (MCNN) for pattern formation. Memristor devices can be integrated into the CNN architecture [2] in a standard way by incorporating their dynamics into the state equation of the CNN cell. We can assume that the default parameter values of the memristor models are obtained by analyzing different charge transportation phenomena. In the investigations of memristor models [3,4], a standard resistor of the RC subcircuit is replaced by a memristor. However, in this case, the well-known internal driving point plot analysis [3], which is applied for the derivation of most of all the templates of standard CNN, cannot be considered. For this reason, second-order cells are realized by taking first-order memristors into account. Applying techniques from the theory of nonlinear dynamics [5] in a comprehensive investigation of cell state equations enables a full characterization of the dynamic behavior of MCNN. Several cell topologies can be obtained by taking different memristor devices into account. The preliminary investigations [4] have shown that new CNN information-processing algorithms with clearly improved calculation efficiency can be derived for non-volatile memristor networks. The variability of circuit elements, especially those of memristors, can be modeled by normal random values and can be assumed in memristor cell simulations to determine admissible variation intervals ensuring local activity in CNN cells. Therefore, if the variability causes locally passive cell behavior, new cell topologies can be derived in order to ensure the emergence of complexity.

The true origin of emergent complexity in nanostructures needs a much deeper new generalization of local activity [6]. The numerous complex phenomena unified under this mathematically precise principle include self-organization, dissipative structures, synergetics, order from disorder, far from thermodynamic equilibrium, collective behavior, edge of chaos, etc. Following the work of Leon Chua [6], in which the theory of local activity is applied to reaction–diffusion CNN, there is only a small number of papers on the generalization of this method for a broader class of CNN. Despite the impressive growth of memristor-related papers [7–38], there are few results on networks of memristive devices. Realized nano-scale CNN have been considered in the investigations dealing with image processing problems [1]. Nano-scale CNN have, so far, been studied via numerical integrations. No analytical results have been derived to date.

This review paper is organized as follows. In Section 2, we present the basic definitions of memristors, together with a survey of their investigations. In this section, we give some basic equations concerning the dynamics of memristors. In Section 3, we make a survey of investigations of CNN. Because of the applications of CNN for pattern generation, which will be discussed later, we shall consider the reaction–diffusion CNN model. Section 4 presents the local activity theory and its applications in studying the dynamics of reaction–diffusion systems. In Section 5, we consider one model of reaction–diffusion memristor cellular nonlinear networks, and we shall study its dynamics by applying the local activity theory. One of the possible applications of MCNN is pattern formation. This is why a short survey on pattern generation in MCNN is provided in Section 6. The main types of patterns arising in the study of MCNN models will be presented.

2. Memristors Basic Definitions

Memristors were introduced by Leon Chua in [7], and, since then, they have become an important emerging element for memory and neuromorphic computing applications (see Figure 1). Novel materials and technologies for these nanostructures [12] have been found and developed for industry. Many mathematical models involving memristors have been presented [13], which reproduce the complex dynamics in nano-devices. For the investigation of the nonlinear dynamics [1] of memristor-based circuits [14,15], it is important to have accurate, general and simple models in order to develop novel hybrid [16] hardware architectures. In this way, memory storage is combined with data processing in the same physical location, which leads to an explanation of the behavior of biological systems. Several physical models have been obtained [17–21] that can study the phenomena characterizing these nano-devices. In [19], some mathematical models of memristors have been presented. Applying mathematical methods, the dynamic behavior of different MCNN models has been studied [31,32,34,35,39]. The first model of a titanium dioxide-based nanostructure was introduced by Williams in [20]. It is a simple model in which the boundary conditions in the state equation are not specified. More complex models appeared after that, in which the nonlinear effects on ionic transport and the definition of the behavior at the boundaries were taken into account. For example, the model proposed by Joglekar in [21] allows only single-valued state flux characteristics under any sign-varying periodic input. In Biolek's model [22], only multi-valued state flux characteristics are considered with the same excitation type. In [23], a comparison of the dynamic behavior of titanium dioxide memristor circuits under different boundary models, such as the BCM model [12], is provided. All these nonlinear circuits are very sensitive to the accuracy of modeling. Moreover, in [20–22], memristor models based on other materials, such as tantalum oxide and niobium dioxide, are developed. In recent investigations, numerical solutions for the strongly nonlinear differential-algebraic equations occur, such as SPICE (Simulation Program with Integrated Circuit Emphasis) simulation [2].

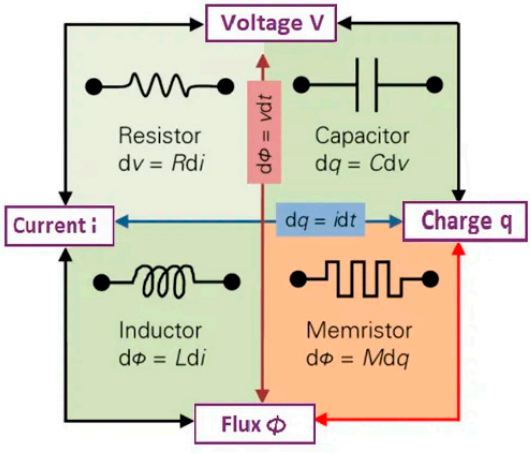

Figure 1. Memristor presentation. Four elements are given: resistor, capacitor, inductor and memristor, with their circuit representations (https://www.britannica.com/technology/memristor).

In order to give completeness to this review paper, we shall introduce memristor dynamics [7,14]. Memristors are invented as single electrical port systems, with the dependence of their conduction properties on the memory of the port variables—current or voltage.

Let us denote, by $\varphi(t)$, the memory of port voltage $v(t)$ by

$$\varphi(t) = \int_{-\infty}^{t} v(\tau)d\tau. \quad (1)$$

In the literature, this is known as voltage momentum or flux [7]. We shall denote, by $q(t)$, the memory of port current $i(t)$

$$q(t) = \int_{-\infty}^{t} i(\tau)d\tau \quad (2)$$

or the current momentum, which physically corresponds to the charge; i is the current. In [7], the ideal memristor is introduced as a bipole with its constitutive relation given by an algebraic equation:

$$F\big(\varphi(t), q(t)\big) = 0$$

We now show the analytical expressions for both a flux-controlled ideal memristor and a charge-controlled ideal memristor:

$$q(t) = f(\varphi(t)) \quad (3)$$

$$\varphi(t) = g(q(t)) \quad (4)$$

Equations (3) and (4) describe the ideal behavior of these two main classes of memristive systems. Let us consider the flux-controlled class (3); then, we can obtain the current–voltage $(i - v)$ expression by means of derivatives of the flux-charge $(\varphi - q)$ with respect to time

$$\frac{dq}{dt} = \frac{df}{d\varphi}\frac{d\varphi}{dt} \quad (5)$$

In (5), we see that $i = \frac{dq}{dt}$ is the current through the bipole, and $v = \frac{d\varphi}{dt}$ is the voltage across its terminals; therefore, it can be rewritten as follows:

$$i(t) = G\big(\varphi(t)\big)v(t) \quad (6)$$

where $G(\varphi)$ is the memductance of the flux-controlled ideal memristor.

If we want to study the dynamics of a larger circuit made of ideal memristors, it is not important that the initial condition of the memristor state variable is explicitly presented in the $(i - v)$ domain.

The formal mathematical definition of the memristor, together with its circuit theoretical properties, is given in [7]. In general, the description of memristor can be described by the system [7]:

$$v = R(x, i)i \quad (7)$$

$$\frac{dx}{dt} = f(x, i) \quad (8)$$

where the voltage across the memristor is denoted by v, the current of the memristor is denoted by i, the state variable is $x = (x_1, x_2, \cdots, x_n)$, which depends on external voltages or currents, and the memristance is $R(x, i)$; $f(x, i)$ is a real function.

As stated at the beginning of this section, in the literature, different memristor models have been proposed. The voltage v–current i relationship expressed by (7) can be found in many of the models in which the control waveform is in current form. When the memristance is presented as the series between two variable resistances, which are associated with the insulating and conductive layers of the nano-film, the state of the system is given in the form $x = \frac{w}{D} \in [0, 1]$. Here, w is the width of the conductive layer, normalized with respect to the entire length, D, of the device. The linear drift model, introduced by Williams in [20], with the time derivative of the state proportional to the input waveform in the current form, is considered under the assumption of low electric fields. It does not take into account the boundary behavior, whereas the nonlinear drift models from [10,11] have the rate of change of the state proportional to the product

between the input waveform in a current form and a window function, accounting for nonlinear dynamical behavior. Suitable boundary conditions are imposed upon it.

3. Cellular Nonlinear Networks

CNN were invented by L. Chua and L. Yang in their papers [1,40] and formed a new class of system that processes information in real-time. Soon after, CNN showed very promissive and important applications [41–43]. CNN copy some properties from neurobiology and are arranged in integrated circuits (see Figure 2). The spatial structure of CNN consists of simple dynamical systems, which are called cells. The state equations of CNN are described by dynamical systems, which present the local dynamic law, the coupling law between the cells. Additionally, there are some initial and boundary conditions. Usually, the cell coupling is considered within the frame of the local neighborhood of each cell. The dynamics of CNN are nonlinear, because they are described by nonlinear ordinary differential equations. Therefore, CNN [42,44] have a very compact representation, given by a system of coupled ordinary differential equations. Nevertheless, CNN can present very complex dynamical behavior, such as chaos, self-organization and pattern formation. Moreover, nonlinear oscillations and wave propagation can appear. Reaction–diffusion CNN [40,45–47] have been studied and applied for modeling different complex phenomena [48–53]. In this way, novel approaches for information processing are developed [2,31–33,35,47,51,54] through the dynamics of complex nonlinear systems.

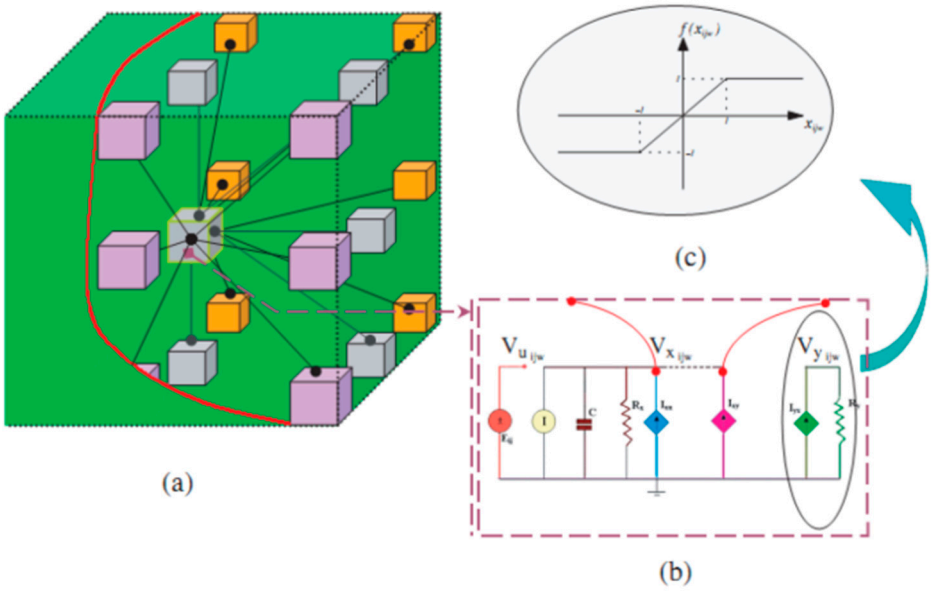

Figure 2. CNN architecture: (**a**) spatial interactions; (**b**) circuit implementation; (**c**) output.

The CNN Universal Machine (CNN-UM) was invented by T. Roska for a single CNN with local and logical memory [41,50,55]. Some time ago, analog CNN-UM chip hardware implementation was developed, as well. In this chip, a parallel computer with stored programmability is included, which allows the possibility for real-time processing of multivariate data. The applications of CNN in image processing and pattern recognition are given in [41,56]. The developed systems, such as the EyeRis 1.3 system, the MIPA4k and SCAMP—5, are mainly sensor-processor systems for high-speed vision, with rates of more than 20 kHz. However, they have low resolution, as, for example, 176X144 pixels in the EyeRis 1.3 system, which makes their application limited in practice. In the future, CNN-UM chip-realization nano-elements can be implemented instead of the conventional CMOS technology, which has a big cell size. In this sense, the memristors [7] with the synaptic connections in the first realization [20] will play a very important role in future

CNN-UM sensor-processor systems. This is because they have complex dynamical behavior. For the development of CNN-based computational methods, it is important to determine the parameter space of the memristor CNN [57,58].

In order to implement a topographic sensory computer, we use the principles from physics or biology. In optics, the spatial correlation is applied at the speed of light. For the construction of the POAC [50]—programmable optoelectronic analogic CNN computer—the 4 f focal plane system using two lenses and a programmable light value is implemented with programmable light transmissivity in each pixel. The POAC laptop realization is shown in Figure 3, in which two different lasers (red and green) are used together with a local analog memory array. The templates are big enough. In this implementation, the nano-devices functions are introduced and defined. In this way, we can produce an array that is locally active, as well as having some sparse global lines by means of optical interconnection.

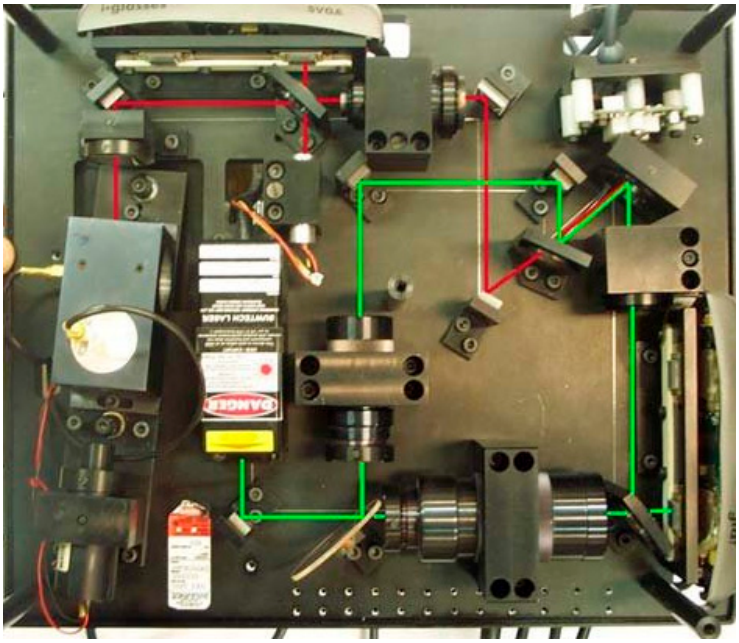

Figure 3. POAC computer [59]. In the picture, a laptop hardware version of the programmable optical analogic array computer (POAC) is shown, which provides high computing speed and full parallelism, having a large input array and template array size.

Such a cellular architecture will be applied in many nano-systems, together with the environment, via acting, communication and sensing. It is better to use some functions of the nano-device that are defined by its layout. In a case when it is locally active, we can make an array and produce local interaction using some sparse global or semi-global lines. This can be obtained via radiation or optical interconnections.

Let us consider the following CNN architecture: a two-dimensional grid with a 3 × 3 neighborhood system, as shown in Figure 4. The cells are represented by squares, and the coupling is presented by straight lines. One possible neighborhood of a cell (in red) is shown by the blue squares and green straight lines, so the red cell has nine possible neighbors [1].

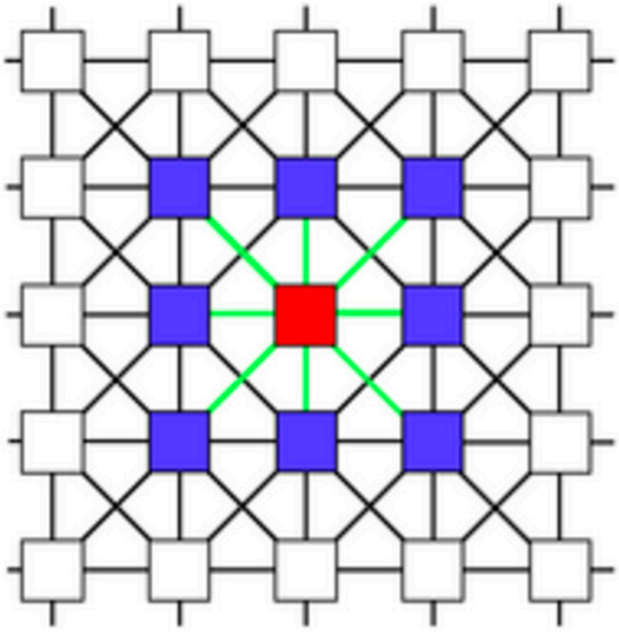

Figure 4. Illustration of the CNN coupling structure.

The cells are denoted by *C(i,j)*, and the links between the cells show the interactions between each cell and its neighbor cells. The dynamics of the cell are presented by nonlinear dynamical systems. The interactions between cells are linear. In this sense, we can consider the CNN as nonlinear systems with linear spatial dynamics [44]. That is why, in the investigation of CNN dynamics, many technics from physics and engineering can be applied.

The dynamics of CNN are described mathematically in [1] by its states equations, which are obtained by applying Kirchhoff's law to the circuit implementation of the CNN given in Figure 2b:

$$\dot{x}_{ij}(t) = -x_{ij}(t) + \sum_{C(k,l)\in N_r(i,j)} \tilde{A}_{ij,kl}(y_{kl}(t), y_{ij}(t)) + \sum_{C(k,l)\in N_r(i,j)} \tilde{B}_{ij,kl}(u_{kl}, u_{ij}) + I_{ij},$$

$$y_{ij}(t) = f(x_{ij}), \tag{9}$$

$$1 \le i \le M, 1 \le j \le M,$$

x_{ij}, y_{ij} and u_{ij} are the state, output and input voltages of a cell $C(i,j)$ and (i,j) denote a grid point associated with a cell on the 2-D grid; $C(k,l) \in N_r(i,j)$ is a grid point (cell) in the neighborhood within a radius, r, of the cell $C(i,j)$; I_{ij} is an independent current source. $\tilde{A}$ and $\tilde{B}$ are nonlinear cloning templates, which specify the interactions between each cell and all its neighboring cells in terms of their input, state and output variables. Reaction–diffusion CNN are usually described by the state equations in which the Laplace operator is approximated by a CNN synaptic law with an appropriate A template:

- a one-dimensional discretized Laplacian template:

$$A_1: (1, -2, 1);$$

- a two-dimensional discretized Laplacian template:

$$A_2: \begin{pmatrix} 0 & 1 & 0 \\ 1 & -4 & 1 \\ 0 & 1 & 0 \end{pmatrix}.$$

As stated before, the most important application of CNN is in image processing [50]. In the one-dimensional case, there are two modes of information propagation existing in

the array: global propagation or local diffusion, meaning that two distant cells do or do not influence each other and determine the corresponding range of coupling parameters. The basic function of CNN for image processing is to map or transform an input image into a corresponding output image. This means that our CNN must always converge to a constant steady state. How can we guarantee the convergence of CNN? There are many studies devoted to finding the conditions which ensure that each trajectory of the network converges to an equilibrium point, depending on the initial conditions [41,42,48,49,55].

Our aim in this review is to consider MCNN and their dynamics, which will be presented in Section 5, in which reaction–diffusion MCNN will be studied. Keeping in mind that there are many works on the theory of MCNN, we aim to give just one example of the mathematical investigation that is based on local activity theory.

4. Local Activity Theory

Complexity phenomena have been studied by many scientists, as well as emergence, self-organization, synergetics, collective behavior nonequilibrium phenomena, etc. [43,56]. In the literature, only qualitative results of different examples from many fields are provided. There is a lack of quantitative results concerning the complex behavior of the systems. In his work, Schrödinger presented the necessary conditions for the complexity of the exchange of energy from open systems. Prigogine [60] introduced a new principle of nature, which he called the instability of the homogeneous. As an origin of morphogenesis, Turing proposed symmetry breaking in [61]. In order to make the Turing interacting system oscillate, Smale [62] tried to find the axiomatic properties of a reaction–diffusion system.

In [6,43,56], mathematical proofs of complexity are presented in order to show that none of the emergent complex behavior in the reaction–diffusion system can be explained without introducing local activity. It is a constructive analytical method for the determination of the edge of chaos region [6]. If we determine the domain of the cell parameters of locally active cells, it is potentially able to exhibit complexity. By rigorous mathematical criteria, emergence and complexity can be explained, which is the main goal of local activity theory and the phenomena edge of chaos. The obtained locally active cell kinetic equations can exhibit complex dynamics, for example, limit cycles or chaos, even if the cells are not coupled with each other. This can be achieved by making all the diffusion coefficients equal to zero. When the cells are coupled, then, complex spatiotemporal phenomena can be observed, for example, scroll waves and spatiotemporal chaos [6,56]. Explicit mathematical inequalities are derived in order to identify the edge of chaos region in the CNN parameter space. If the cell parameter space is in the local activity domain, then the computation time for the parameter search algorithms can be reduced [43,56]. For different CNN models, the edge of chaos domain is obtained in the investigations. In [47,54], reaction–diffusion CNN models are considered, and the domain of the cell parameters for locally active cells is obtained, in which they can exhibit complexity.

5. Memristor Cellular Nonlinear Networks and Their Dynamics

Different models of memristive nanostructures have been studied [2,12,23,27–29,36,37,42]. The investigations into the implementation of memristors in integrated circuit design include some of the most common learning rules based on brain functionalities. Optimized mathematical models have been made to capture the dynamics when the parameters of the Pickett model are fitted to experimental data. In [30] a polynomial model (PM) for a niobium-dioxide-based memory device was introduced. In this model, the memductance and the state evolution function are represented by a polynomial following the unfolding theorem [25]. The coefficients of the polynomial series need to be fitted to the reference model based on the given circuit and excitation.

We shall integrate the memristor dynamics of (7) and (8) into a general reaction–diffusion model. The well-known reaction–diffusion (RD) equation is

$$\frac{\partial u}{\partial t} = g(u) + D\,\nabla^2 u,$$

where $u \in \boldsymbol{R}^n$, $g \in \boldsymbol{R}^n$, D is a matrix with diffusion coefficients and ∇^2 is the Laplacian operator in $\boldsymbol{R}^2$. Instead of resistors for diffusion in analog RD large-scale integrators (LSIs), we shall introduce memristors.

Let $u(x)$ be represented by voltages on the RD-CNN hardware; then, the diffusion terms in the RD model are represented by linear resistors. We shall discretize the Laplacian ∇^2 as

$$\nabla^2 u(x) = \frac{u_{i-1} + u_{i+1} - 2u_i}{\Delta x^2}$$

where Δx is the discrete step in space.

Generally, we shall consider the RD system described by:

$$\frac{\partial\, u(x)}{\partial\, t} = g_u\ \nabla^2 \mathrm{u(x)} + f_u(u(x),\ v(x))$$

$$\frac{\partial\, v(x)}{\partial\, t} = g_v\ \nabla^2 \mathrm{u(x)} + f_v(u(x),\ v(x))$$

where $g_{u,v}$ are the diffusion coefficients, and $f_{u,v}(.)$ are the functions of the states for the reaction model.

In the RD system, *u(x)* and *v(x)* are represented by voltages on the RD hardware, and the gradient is represented by linear resistors. We apply, below, one-dimensional spatial discretization.

We discretize spatially the first equation of the RD system in the following way:

$$\frac{d\, u_j(t)}{dt} = \frac{g_u(u_{j-1} - u_j) + g_u(u_{j+1} - u_j)}{\Delta x^2} + f_u(.), \tag{10}$$

where, by *j*, the spatial index is denoted, Δx is the discrete step in space, terms $g_u(u_{j-1} - u_j)$ and $g_u(u_{j+1} - u_j)$ represent, respectively, the current flowing into the *j*th node from the *(j − 1)*th and *(j + 1)*th nodes via two resistors whose conductance is represented by g_u. Here, we introduce the memristor model, in which the resistors are replaced with memristors. The resulting point dynamics are given by

$$\frac{d\, u_j}{d\, t} = \frac{g_u(w_j^l)(u_{j-1} - u_j) + g_u(w_j^r)(u_{j+1} - u_j)}{\Delta x^2} + f_u(.), \tag{11}$$

where $g_u(.)$ denotes the monotonically increasing function defined by:

$$g_u(w_j^{l,r}) = g_{min} + (g_{max} - g_{min})\ \frac{1}{1 + e^{-\beta w_j^{l,r}}},$$

where β denotes the gain, g_{min} and g_{max} denote the minimum and maximum coupling strengths, respectively, and $w_j^{l,r}$ denotes the variables for determining the coupling strength (*l*—leftward, *r*—rightward).

Finally, we introduce the following memristive dynamics for $w_j^{l,r}$:

$$\tau \frac{dw_j^{l,r}}{dt} = g_u(w_j^{l,r}).\eta_1.(u_{j-1} - u_j), \tag{12}$$

where the right-hand side represents the current of the memristors, and η_1 denotes the polarity coefficient—$\eta_1 = +1$: w_j^l, $\eta_1 = -1$: w_j^r.

As an example, we shall consider the Oregonator CNN model [9]:

$$\frac{du_{ij}}{dt} = D_1 A_2 * u_{ij}(1-u_{ij}) - av_{ij}\frac{u_{ij}-b}{b+u_{ij}} = G_1(u_{ij}, v_{ij})$$
$$\frac{dv_{ij}}{dt} = D_2 A_2 * v_{ij} + u_{ij} - v_{ij} = G_2(u_{ij}, v_{ij}) \quad (13)$$

According to the above theory, we shall incorporate memristor dynamics in the Oregonator CNN model in the following way:

$$\frac{du_{ij}}{dt} = D_1(w_{ij}^{l,r})A_2 * u_{ij}(1-u_{ij}) - av_{ij}\frac{u_{ij}-b}{b+u_{ij}} = G_1(u_{ij}, v_{ij})$$
$$\frac{dv_{ij}}{dt} = D_2(w_{ij}^{l,r})A_2 * v_{ij} + u_{ij} - v_{ij} = G_2(u_{ij}, v_{ij}) \quad (14)$$

We present the Oregonator model, above, because we shall study a new reaction–diffusion-type excitable medium. The Oregonator describes the kinetic chemical reaction model of morphogenesis.

We apply a constructive algorithm for the determination of the locally active region and the edge of chaos in our model [6]. First, we find the equilibrium points of (14), i.e., $G_1(u_{ij}, v_{ij}) = 0$ and $G_2(u_{ij}, v_{ij}) = 0$. We obtain three equilibrium points: $E_1 = (0,0), E_2 = (b,b)$, and $E_3 = (-b,-b)$. Then, we find the four cell coefficients: a_{11}, a_{12}, a_{21} and a_{22}. The locally active region for each equilibrium point can be defined as follows:

$$LAR(E_p):\ a_{22} > 0, or\ 4a_{11}a_{22} < (a_{12} + a_{21})^2$$

An additional stability condition in this case is:

$$Tr(E_p) < 0\ and\ D(E_p) > 0.$$

After checking the above conditions, we obtain the following results: In the equilibrium point $E_1 = (0,0)$, we have a stable and locally active region; in the equilibrium points $E_2 = (b,b)$, and $E_3 = (-b,-b)$, we obtain unstable regions. The simulation of the above analysis is presented in Figure 5 below:

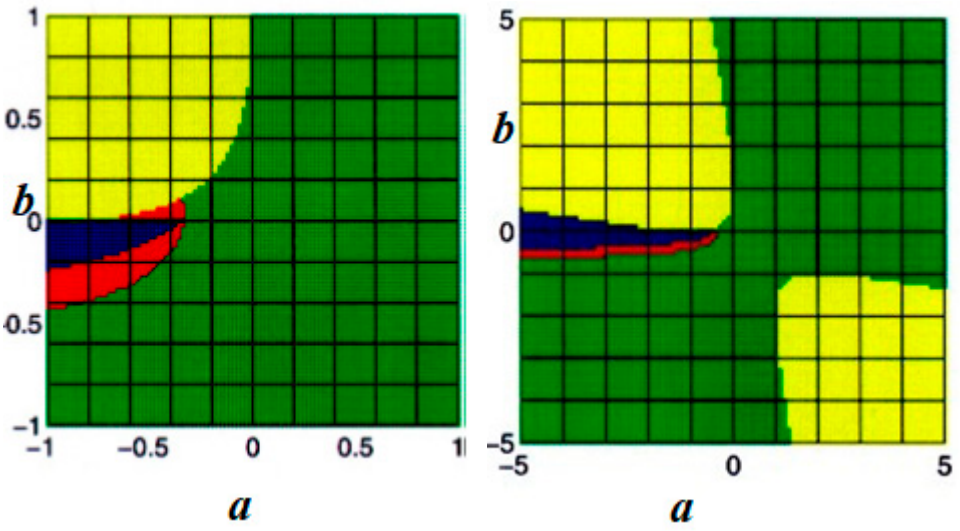

Figure 5. Bifurcation diagrams of the Oregonator model for different sets of cell parameters. The edge of chaos region is shown in red, the locally active and unstable region is given in green, and the locally passive region is blue. In the domain coded with yellow, no equilibrium point exists.

Some comments on the results obtained in Figure 5 follow: For the numerical simulations, we should have information for the behavior of the solutions. One advantage

of the above algorithm is its robustness. Therefore, we are able to calculate all the necessary processing steps in real-time due to the MCNN programmable realization. Our simulations shown in Figure 5 are obtained via MATLAB simulations based on the fourth-order Runge–Kutta integration.

The results we obtain after simulating of Oregonator model (14) are as follows:

(1) the Oregonator model exhibits limit-cycle oscillations and excitatory behaviors, which depend on the reaction parameters;
(2) non-uniform spatial-pattern generation is observed, which depends on the initial condition of the Oregonator's state, memristor polarity and stimulation.

This will be shown and commented on in Section 6, below. The answer to the question: "what happens if one replaces resistors in analog RD LSIs with memristors?" will be given.

6. Applications of MCNN for Pattern Formation

In this section, we present an application of MCNN considered in the previous section to pattern generation. It is important to point out that the following analysis is based on the local activity theory [6]. We consider the reaction–diffusion model in our investigation.

Dynamical systems arising in engineering, biology, fluids, chemistry and plasmas can develop various patterns. The formation of patterns in hydra was described in the famous paper by Turing [61]. There are many patterns in nature, such as seashells [63] and animal coats [64], which are modeled by the dynamics of spatial pattern formation. The mechanism for fingerprints [65] is described by methods of pattern generation in engineering.

Pattern generation is usually studied theoretically, experimentally or via simulations. Direct evidence of reaction–diffusion in physical systems is studied experimentally, but it is difficult to control the parameters in these cases. The evolution of the dynamics in chemical and biological substrates is very slow. In order to find insights into the effects, we must vary the parameters for controlling the reaction and diffusion components arbitrarily, by means of theoretical and simulation studies. These investigations are quite long because of the modeling assumptions, such as approximations and discretization in time and amplitude.

According to the definition given in [6], MCNN are working in the edge of chaos (EC) domain if we can find at least one equilibrium point in the locally active and stable region. Depending on the parameters, it is possible to obtain different patterns in the EC domain. In the case when there is only one diffusion coefficient in the EC region, static patterns are generated. With two diffusion coefficients, it is possible for Turing-like static patterns to develop. In this case, the coupling coefficient should be taken, depending on the location of the cell parameter point in the boundary region between the locally active and unstable domain and the EC domain. It is known that Turing-like patterns can be generated in CNN when the cells are in the EC region only for the two-diffusional case. Then, the possibility of the emergence of complexity [6] is very high when the cell parameters are in the EC domain in both the one-diffusion and two-diffusion cases.

Below, in Figures 6–9, different kinds of patterns generated in MCNN models under consideration are given.

In Figure 6, Turing patterns arising in a reaction–diffusion system are generated when the dynamical system is changed by replacing $u^2 \to \frac{u^2}{1+ku^2}$. In this case, with the change of the parameter, k, Turing instability occurs, and we obtain the variety of patterns shown in the figure. In the simulations λ, μ and ρ are the parameters of the RD system.

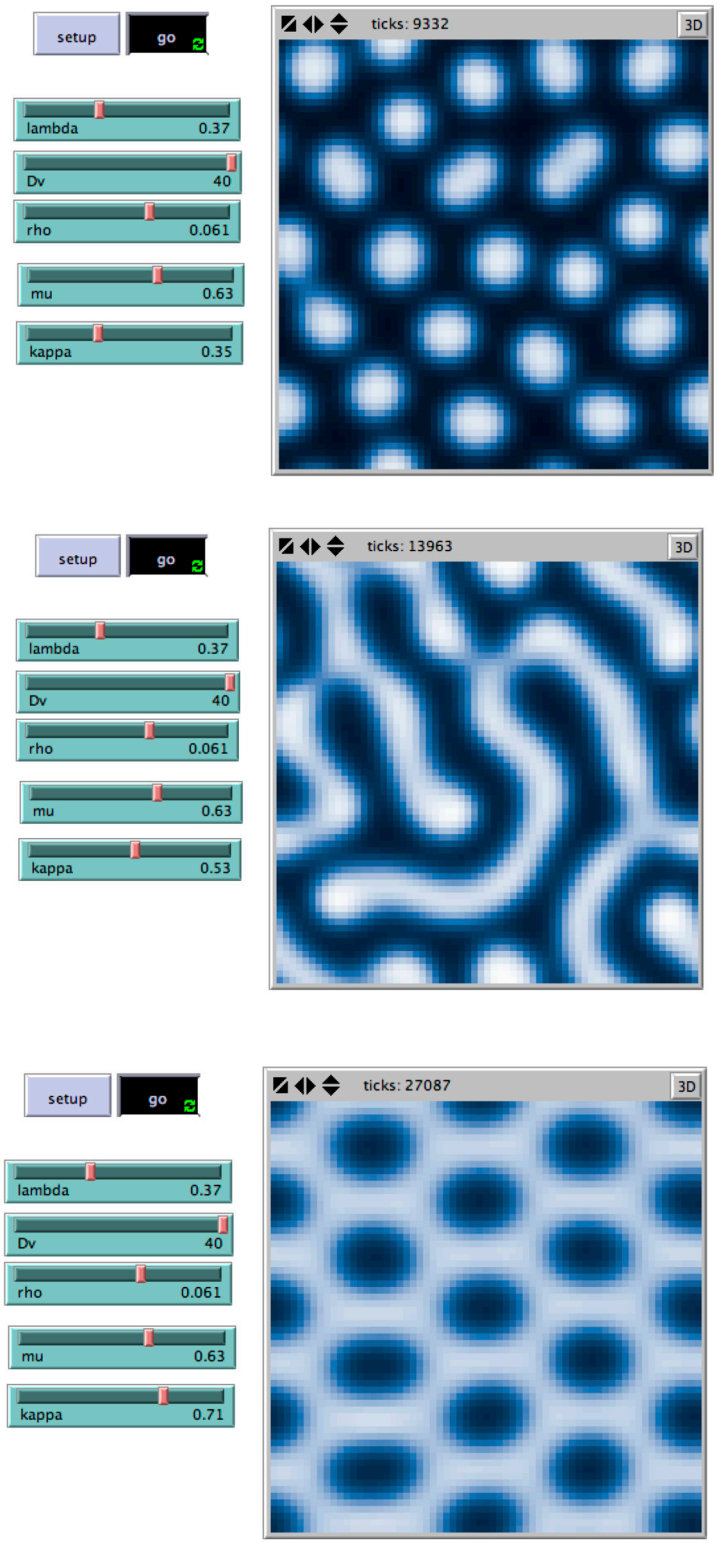

Figure 6. Turing patterns in reaction–diffusion MCNN. When the parameter, *k*, is changed, different patterns are obtained.

As we pointed out in Section 5 for the Oregonator MCNN model, we can determine the edge of chaos domain of the parameter sets in which complex behavior can emerge. Nonuniform spatial patterns are generated in this model, and they are presented in Figure 7. The initial state of all the Oregonator cells is set to be the inactive state. After stimulating the center node, the excitable waves propagated outwards, as shown in Figure

8. Among the demonstrated behaviors, the nonuniform spatial-pattern generation is applied to investigations detecting the pattern generation due to the memristors. Therefore, if one has proper (non-memristive) RD media and a 2-D array of memristors without any reaction circuit, and the point dynamics of the RD media are given to the memristor array, one may detect the global motions of the RD media. This application is not limited to the analysis of RD systems, but the idea can be transferred to analyzing much more complex systems, such as brain networks, social networks and so on.

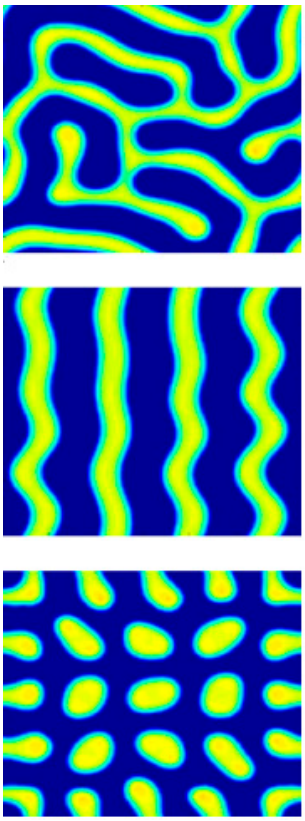

Figure 7. Pattern formation in the Oregonator model studied in Section 5, depending on the initial condition of Oregonator's state, memristor polarity and stimulation.

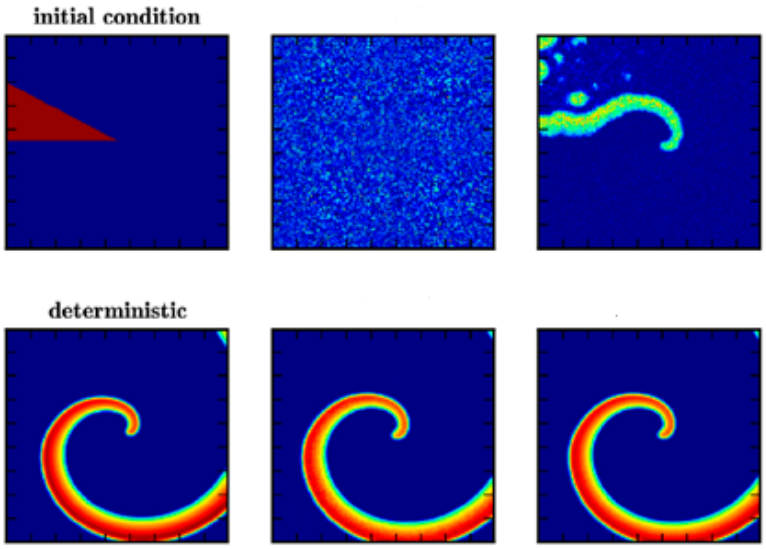

Figure 8. Spiral waves obtained when the point dynamics of the RD media of the Oregonator MCNN model are applied to the memristor array.

After the simulations of the Oregonetor model presented in Figures 7 and 8, we make the following conclusions: (a) the memristor's conductances are modulated by excitable waves propagating on the memristor, depending on the memristor's polarity; and (b) the velocity of the excitable wave propagation is thus modulated by the change of memristor conductance, and the degree of the modulation is inversely proportional to the time constant of the memristor's model.

Dynamic patterns are usually obtained [6] within the locally active and unstable region. Complex behavior can emerge when the cell parameter points are located on the boundary between the edge of chaos region and the locally active and unstable region [6]. In this sense, the chaotic dynamic patterns, presented in Figure 9, are generated for the cell parameter points. Usually, they are very close to the edge of chaos region and within the locally active and unstable region. According to the local activity theory [6], when the cell parameter points are within the locally passive region, complex behavior is observed in MCNN, with some particular cases when the initial conditions are near the equilibrium point. Usually, the stability analysis does not give the exact cell parameter domain in which the cells are locally passive [6]. Two kinds of pseudo-color codes were introduced to graphically exhibit the complex dynamic behavior of the Oregonator array. Extensive computer simulations have tested the effectiveness of the local activity theory and have displayed the extremely complex behavior of the cells of the reaction–diffusion array equations.

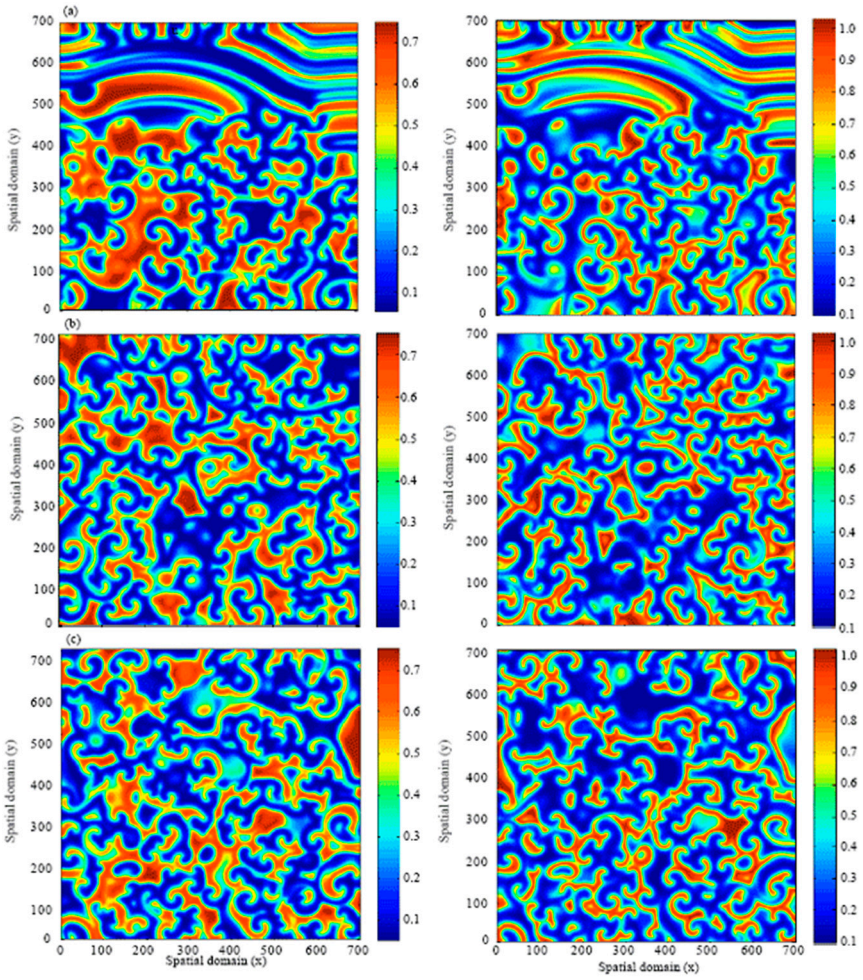

Figure 9. Chaotic patterns arising in the locally active and unstable region on the boundary of the edge of chaos region for different cell parameter sets.

It is well known [65] that some complex systems can self-organize into spatially structured states independent of the initial states, which can be unstructured or spatially homogeneous. Such phenomena are observed in all scientific fields, for example, in physics, biology, social science, etc. In order to explain how such behavior occurs, we need some explanation. The experimental simulations are close to the behavior observed in the associated set of reaction–diffusion equations. By applying our theoretical analysis of MCNN, which is provided for the example of the Oregonator system, we can predict with accuracy the dependence of the experimental measures of the obtained patterns on the input parameters. By studying the two-layer MCNN, we can understand better the pattern formation dynamics of the chip. In this case, we have a stable diffusion process, which results in the evolution of such an array of different spatial patterns.

As a conclusion to this section, we would like to point out that oscillatory patterns, static (convergent) patterns and unbounded (divergent) patterns can be formed only in cases where the parameter set is determined in the edge of chaos domain. In some particular cases, complex patterns can be generated if the cell parameters are in the locally active unstable domain, but in the border of the edge of chaos domain. This proves that the local activity theory gives us an explicit analytical method for the study of complexity.

7. Discussion

There are many models of physical, chemical and biological systems using CNN architecture. Because of its continuous-time analog operation, it is possible to provide real-time signal processing with high precision. This is due to the local interconnection between the processing elements, which leads to several digital and analog implementations of CNN architecture in the form of very large-scale integrated chips (VLSI). Several powerful applications for CNN are reported in the literature, which include pattern and image analysis, such as vertical line detection, noise reduction, edge detection, feature detection, character recognition, etc. [41–43,45,46,48–50,55].

In order to improve the resolution in static and dynamic image processing, it is necessary to reduce the size of the processing elements and the connectivity between these elements describing the feedforward and feedback templates in the CNN models. It is known that the current versions of CNN arrays in CMOS VLSI chips are limited to 16K processing elements [66,67]. Recently, some new technologies, such as resonant-tunneling diode and quantum dots, implement processing elements in a more compact way to improve the resolution of CNN computation. For example, in [68], it is shown that photo-reversible photochromic compounds are presented and used for the implementation of optical synapsis and memory effects which improve pattern recognition significantly. The introduction of memristors offers the possibility to significantly enhance the resolution of the CNN model of computation [69,70]. The main properties of memrsitors (nonvolatility, binary and multiple memory states and nanometer geometries) are important for nanofabrication technology. These promising properties of memristors have been exploited in their applications in nonvolatile memory, artificial neural networks, etc. [71–74]. Their conductance can change in response to the applied voltage or current like a biological synapse, and that is why they are applied for biological signal processing. In [4,38], a compact memristor bridge synapse is presented in order to perform weighting and weight programming at different time slots. All resistive switching devices can be modeled by mapping the physical processes that underpin their operation to the memristive framework. The key is in identifying a state variable that accurately captures the important aspects of the system and then describing its dynamic, time evolution in response to the memristor's inputs. The first use of the memristive framework was to describe resistive switching, characterizing the behavior of TiO2 devices. Here, the memristor was composed of two adjacent regions, doped and undoped, with oxygen vacancies, with a movable boundary between the regions while keeping the overall film thickness fixed.

Memristor devices have a two-terminal nature and the ability to change conductance when they are stimulated with voltage pulses and evolve into states which are based on the input history. For this reason, they become almost ideal electronic analogies of the biological synapses. Moreover, since memristors can be implemented in a crossbar architecture, they are adaptive, with high density and large connectivity which leads to neuromorphic applications. Memristors can store a static weight as an analog resistance value, unlike the conventional artificial neural networks, which offer more complex internal dynamics, and, in this way, they can be used to implement different bio-mimicking learning rules. Memristors can be applied to the direct implementation of learning rules, which is a very challenging approach.

8. Conclusions

In this paper, we present a review of memristor cellular nonlinear networks from the point of view of the theory and applications. We discuss the developments in both fields—memristors and cellular nonlinear networks. Then, we present, as an example, an MCNN model of the Oregonator system, and we apply local activity theory in order to study its dynamics. The locally active domain of the parameter space of this model is determined, as well as the edge of chaos region. A short presentation of the pattern formation in MCNN models is presented at the end of the paper, showing a possible application. The solutions calculated in these models can be compared to those of known phenomena in excitable media. Furthermore, different excitations are applied to generate non-uniform spatial patterns, depending also on the initial condition of the CNN cell state and the memristor polarity.

The local activity theory for reaction–diffusion equations could be generalized to other systems. In particular, it is applicable to any system whose cells and couplings are described by deterministic mathematical models. In such generalizations, it is very important to derive testable necessary and sufficient conditions, which guarantee that the system has a unique steady-state solution at t→∞. In the case of equilibrium states, each cell must be defined by a strictly monotone increasing function of the port state variables. The fact is that a strictly monotone increasing function imposes stronger mathematical conditions than a homeomorphic function in R^n, $n \geq 2$. One can interpret this definition as a generalization of the concept of a strictly monotone increasing function to the function space. The general conditions for the case n>2 are obtained during the simulation procedure of reaction–diffusion MCNN and can be based on the following conjecture: A homogeneous non-conservative medium cannot exhibit complexity unless the cell or the coupling network is locally active.

Funding: This research received no external funding.

Acknowledgments: The authors acknowledge the grant, "Machine learning through physics—informed neural networks" KP-06-N 62/6.

Conflicts of Interest: The authors declare no conflict of interest.

References

1. Chua, L.; Yang, L. Cellular neural networks: Theory. *IEEE Trans. Circuits Syst.* **1988**, *35*, 1257–1272. https://doi.org/10.1109/31.7600.
2. Tetzlaff, R. *Memristor and Memristive Systems*; Springer: Berlin/Heidelberg, Germany, 2014.
3. Loroch, D.M. Study and Analysis of CNN with Real Memristor Devices. Diploma Thesis, Dresden, 2016.
4. Duan, S.; Hu, X.; Dong, Z.; Wang, L.; Mazumder, P. Memristor-Based Cellular Nonlinear/Neural Networks: Design, Analysis, and Applications. *IEEE Trans. Neural Netw. Learn. Syst.* **2015**, *26*, 6.
5. Chua, L.O. *Introduction to Nonlinear Network Theory*; McGraw-Hill Series in Electronic Systems; 1969.
6. Chua, L.O. Local activity is the origin of complexity. International Journal of Bifurcation and Chaos 2005, 15, No. 11, 3435-3456.
7. Chua, L. Memristor-The missing circuit element. *IEEE Trans. Circuit Theory* **1971**, *18*, 507–519. https://doi.org/10.1109/tct.1971.1083337.

8. Mikolajick, T. *From Basic Switching Mechanism to Device Applications*; DATE, Workshop on Memristor Science & Technology: Dresden, Germany, 2014.
9. Corinto, F.; Ascoli, A. A Boundary Condition-Based Approach to the Modeling of Memristor Nanostructures. *IEEE Trans. Circuits Syst. I Regul. Pap.* **2012**, *59*, 2713–2726. https://doi.org/10.1109/tcsi.2012.2190563.
10. Corinto, F.; Ascoli, A.; Gilli, M. Nonlinear Dynamics of Memristor Oscillators. *IEEE Trans. Circuits Syst. I Regul. Pap.* **2011**, *58*, 1323–1336. https://doi.org/10.1109/tcsi.2010.2097731.
11. Talukdar, A.; Radwan, A.G.; Salama, K.N. Nonlinear dynamics of memristor based 3rd order oscillatory system. *Microelectron. J.* **2012**, *43*, 169–175.
12. Ascoli, A.; Corinto, F.; Tetzlaff, R. Generalized boundary condition memristor model. *Int. J. Circuit Theory Appl.* **2015**, *44*, 60–84. https://doi.org/10.1002/cta.2063.
13. Strukov, D.B.; Stewart, D.R.; Borghetti, J.L.; Li, X.; Pickett, M.; Ribeiro, G.M.; Robinett, W.; Snider, G.S.; Strachan, J.P.; Wu, W.; et al. Hybrid CMOS/memristor circuits. In Proceedings of the 2010 IEEE International Symposium on Circuits and Systems (ISCAS), Paris, France, 30 May–2 June 2010; pp. 1967–1970.
14. Chua, L.O. The fourth element. *Proc. IEEE* 2012, 100, 1920–1927.
15. Kvatinsky, S.; Friedman, E.G.; Kolodny, A.; Weiser, U.C. TEAM: ThrEshold Adaptive Memristor Model. *IEEE Trans. Circuits Syst. I: Regul. Pap.* **2012**, *60*, 211–221. https://doi.org/10.1109/tcsi.2012.2215714.
16. Pickett, M.D.; Strukov, D.B.; Borghetti, J.L.; Yang, J.J.; Snider, G.S.; Stewart, D.R.; Williams, R.S. Switching dynamics in titanium dioxide memristive devices. *J. Appl. Phys.* **2009**, *106*, 074508. https://doi.org/10.1063/1.3236506.
17. Pickett, M.D.; Williams, R.S. Sub-100 fJ and sub-nanosecond thermally driven threshold switching in niobium oxide crosspoint nanodevices. *Nanotechnology* **2012**, *23*, 215202.
18. Strachan, J.P.; Torrezan, A.C.; Miao, F.; Pickett, M.D.; Yang, J.J.; Yi, W.; Medeiros-Ribeiro, G.; Williams, S. State Dynamics and Modeling of Tantalum Oxide Memristors. *IEEE Trans. Electron Devices* **2013**, *60*, 2194–2202. https://doi.org/10.1109/ted.2013.2264476.
19. Ascoli, A.; Tetzlaff, R.; Biolek, Z.; Kolka, Z.; Biolkova, V.; Biolek, D. The Art of Finding Accurate Memristor Model Solutions. *IEEE J. Emerg. Sel. Top. Circuits Syst.* **2015**, *5*, 133–142. https://doi.org/10.1109/jetcas.2015.2426493.
20. Strukov, D.B.; Snider, G.S.; Stewart, D.R.; Williams, R.S. The missing memristor found. *Nature* **2008**, *453*, 80–83. https://doi.org/10.1038/nature06932.
21. Joglekar, Y.N.; Wolf, S.T. The elusive memristive element: properties of basic electrical circuits. *Eur. J. Phys.* **2009**, *30*, 661–675.
22. Biolek, Z.; Biolek, D.; Biolkovà, V. Spice model of memristor with nonlinear dopant drift. *Radio Eng.* **2009**, *18*, 210–214.
23. Ascoli, A.; Corinto, F.; Senger, V.; Tetzlaff, R. Memristor Model Comparison. *IEEE Circuits Syst. Mag.* **2013**, *13*, 89–105. https://doi.org/10.1109/mcas.2013.2256272.
24. Torrezan, A.C.; Strachan, J.P.; Medeiros-Ribeiro, G.; Williams, R.S. Sub-nanosecond switching of a tantalum oxide memristor. *Nanotechnology* **2011**, *22*, 485203. https://doi.org/10.1088/0957-4484/22/48/485203.
25. Ascoli, A.; Slesazeck, S.; Mahne, H.; Tetzlaff, R.; Mikolajick, T. Nonlinear Dynamics of a Locally-Active Memristor. *IEEE Trans. Circuits Syst. I Regul. Pap.* **2015**, *62*, 1165–1174. https://doi.org/10.1109/tcsi.2015.2413152.
26. Ascoli, A.; Lanza, V.; Corinto, F.; Tetzlaff, R. Synchronization conditions in simple memristor neural networks. *J. Frankl. Inst.* **2015**, *352*, 3196–3220. https://doi.org/10.1016/j.jfranklin.2015.06.003.
27. Cai, W.; Tetzlaff, R. Advanced memristive model of synapses with adaptive thresholds. In *International Workshop on Cellular Nanoscale Networks and Their Applications (CNNA)*; IEEE: Turin, Italy, 2012.
28. Ascoli, A.; Tetzlaff, R.; Corinto, F.; Gilli, M. PSpice switch-based versatile memristor model. In Proceedings of the 2013 IEEE International Symposium on Circuits and Systems (ISCAS2013), Beijing, China, 19–23 May 2013; pp. 205–208. https://doi.org/10.1109/ISCAS.2013.6571818.
29. Cai, W.; Tetzlaff, R. Synapse as a Memristor. In *Memristor Networks*; Springer: Berlin/Heidelberg, Germany, 2014; pp. 113–128.
30. Ascoli, A.; Slesazeck, S.; Tetzlaff, R.; Meahne, H.; Mikolajick, T. Unfolding the local activity of a memristor. In *International Workshop on Cellular Nanoscale Networks and Their Applications (CNNA)*; IEEE: Piscataway, NJ, USA, 2014.
31. Slavova, A.; Tetzlaff, R. Edge of chaos in reaction diffusion CNN model. *Open Math.* **2017**, *15*, 21–29. https://doi.org/10.1515/math-2017-0002.
32. Slavova, A.; Tetzlaff, T. *Mathematical Analysis of Memristor CNN*. ItechOpen: London, UK, 2019. https://doi.org/10.5772/intechopen.86446.
33. Slavova, A. Local activity in reaction-diffusion CNN models. *AIP Conf. Proc.* **2019**, *2159*, 030030-1-11. https://doi.org/10.1063/1.5127495.
34. Slavova, A.; Zafirova, Z.; Tetzlaff, R. Edge of Chaos in Nanoscale Memristor CNN. In Proceedings of the 2019 IEEE International Symposium on Circuits and Systems (ISCAS), Sapporo, Japan, 26–29 May 2019. https://doi.org/10.1109/iscas.2019.8702436.
35. Slavova, A.; Tetzlaff, R. Edge of Chaos in Memristor CNN with Hysteresis and Applications in Pattern Formation. In Proceedings of the 2021 IEEE International Symposium on Circuits and Systems (ISCAS), Daegu, Korea, 22–28 May 2021. https://doi.org/10.1109/iscas51556.2021.9401334.
36. Corinto, F.; Ascoli, A. Memristive diode bridge with LCR filter. *Electron. Lett.* **2012**, *48*, 824–825. https://doi.org/10.1049/el.2012.1480.
37. Ascoli, A.; Corinto, F.; Tetzlaff, R. A class of versatile circuits, made up of standard electrical components, are memristors. *Int. J. Circuit Theory Appl.* **2015**, *44*, 127–146. https://doi.org/10.1002/cta.2067.

38. Kim, H.; Sah, M.; Yang, C.; Roska, T.; Chua, L.O. Memristor Bridge Synapses. *Proc. IEEE* **2012**, *100*, 2061–2070.
39. Corinto F.; Forti M. Memristor Circuits: Flux—Charge Analysis Method. *IEEE Trans. Circuit Syst. I* **2016**, *63*, 1997–2009.
40. Chua, L.O.; Yang, L. CNN: Applications. *IEEE Trans. Circuits Syst.* **1988**, *35*, 1273–1299.
41. Chua, L.O.; Roska, T. *Cellular Neural Networks and Visual Computing—Foundations and Applications*; Cambridge University Press: Cambridge, UK, 2001.
42. Hanggi, M.; Moschytz, G. *Cellular Neural Networks: Analysis, Design and Optimization*; Kluwer Academic Publishers Pub.: Germany, 2000.
43. Manganaro, G.; Arena, P.; Fortuna, L. *Cellular Neural Networks: Chaos, Complexity and VLSI Processing*; Springer Verlag: Berlin/Heidelberg, Germany, 1999.
44. Slavova, A. *Cellular Neural Networks: Dynamics and Modelling*; Mathematical Modelling: Theory and Applications 16; Kluwer Academic Publishers: 2003.
45. Dogaru, R. *Universality and Emergent Computation in Cellular Neural Networks*; World Scientific: Singapore, 2003.
46. Slavova, A. Stabilization of coupled reaction-diffusion CNN. In Proceedings of the 2013 European Conference on Circuit Theory and Design (ECCTD), Dresden, Germany, 8–12 September 2013; p. 101. https://doi.org/10.1109/ecctd.2013.6662311.
47. Slavova, A.; Rashkova, V. Edge of chaos in reaction-diffusion CNN models. In *Mathematical Analysis, Differential Equations and Their Applications*; Academic Publishing House "M.Drinov": 2011; Volume 207–216, p. 2011.
48. Special issue on CNN. *Int. J. Circuit Theory Appl.* **1992**, *20*.
49. Special issue on Chaos. *IEEE Trans. CAS-I* **1995**, *42*.
50. Roska, T.; Rodríguez-Vázquez, A. *Toward the Visual Microprocessor-VLSI Design and the Use of Cellular Neural Network (CNN) Universal Machine Computers*; J. Wiley: London, UK, 2001.
51. Slavova, A. Applications of some mathematical methods in the analysis of cellular neural networks. *J. Comput. Appl. Math.* **2000**, *114*, 387–404. https://doi.org/10.1016/s0377-0427(99)00277-0.
52. Slavova, A.; Tetzlaff, R.; Markova, M. CNN computing of the interaction of fluxons. In Proceedings of the 2011 URSI General Assembly and Scientific Symposium, Istanbul, Turkey, 13–20 August 2011.
53. Slavova, A.; Tetzlaff, R. CNN computing of double Sine-Gordon equation with physical applications. *C. R. Bulg. Acad. Sci.* **2014**, *67*, 21–28.
54. Slavova, A. Chaotic Behavior of Hysteresis Cellular Nonlinear Networks and its Control. *Proc. NDES, Dresden, Germany* 2010, 74–77.
55. Roska, T.; Vandewalle, J. (Eds.) *Cellular Neural Networks*; Wiley, John & Sons, Incorporated Pub.: Hoboken, NJ, USA, 1994.
56. Chua, L.O. *CNN: A Paradigm for Complexity*; World Scientific Pub Co.: Singapore, 1998.
57. Schetzen, M. *The Volterra and Wiener Theories of Nonlinear Systems*; Revised edition; Krieger Publishing Company: Spain, 2006.
58. Kunz, R.; Tetzlaff, R.; Wolf, D. SCNN: a universal simulator for cellular neural networks. In Proceedings of the 1996 Fourth IEEE International Workshop on Cellular Neural Networks and their Applications Proceedings (CNNA-96), Seville, Spain, 24–26 June 1996. https://doi.org/10.1109/cnna.1996.566570.
59. Available online: www.lab.analogic.sztaki.hu (accessed on 20 January 2023).
60. Prigogine, I. *From Being to Becoming: Time and Complexity in the Physical Sciences*; W.H.Freeman: San Francisco, CA, USA, 1980.
61. Turing, A.M. The chemical basis of morphogenesis. *Phil. Trans. Royal Soc. B* **1952**, *237*, 37–72.
62. Smale, S. A mathematical model of two cells via Turing's equation. *Lect. Appl. Math.* **1974**, *6*, 15–26.
63. Meinhardt, H. *The Algorithmic Beauty of Sea Shells*; Springer-Verlag: Berlin, Germany, 1995.
64. Murray, J.D. *Mathematical Biology*, 2nd ed.; Springer: Berlin, Germany, 1993.
65. Crounse K.R.; Chua, L.O. Methods for image processing and pattern formation in cellular neural networks: A tutorial. *IEEE Trans. Circuit Syst. I* **1995**, *42*, 583–601.
66. Rodríguez-Vázquez, A.; Domínguez-Castro, R.; Jiménez-Garrido, F.; Morillas, S. A CMOS Vision System On-Chip with Multicore Sensory Processing Architecture for Image Analysis above 1,000 F/s. *Sens. Cameras Syst. Ind.-Al/Sci. Appl. XI* **2010**, *7536*, 213–223.
67. Laiho, M.; Poikonen, J.; Paasio, A. MIPA4k: Mixed-Mode Cellular Processor Array. *Focal-Plane Sensor-Processor Chips*; Springer: Berlin/Heidelberg, Germany, 2011. https://doi.org/10.1007/978-1-4419-6475-5_3.
68. Gentili, P.L.; Giubila, M.S.; Germani, R.; Heron, B.M. Photochromic and luminescent compounds as artificial neuron models. *Dye. Pigment.* **2018**, *156*, 149–159. https://doi.org/10.1016/j.dyepig.2018.04.006.
69. Tetzlaff R.; Ascoli, A.; Messaric, I.; Chua, L. Theoretical Foundations of Memristor Cellular Nonlinear Networks: Memcomputing With Bistable-Like Memristors. *IEEE Trans. Circuits Syst. I Reg. Pap.* **2020**, *67*, 502–515.
70. Di Marco, M.; Forti, M.; Pancioni, L. Memristor standard cellular neural networks computing in the flux–charge domain. *Neural Networks* **2017**, *93*, 152–164. https://doi.org/10.1016/j.neunet.2017.05.009.
71. Lin, H.; Wang, C.; Deng, Q.; Xu, C.; Deng, Z.; Zhou, C. Review on chaotic dynamics of memristive neuron and neural network. *Nonlinear Dyn.* **2021**, *106*, 959–973. https://doi.org/10.1007/s11071-021-06853-x.
72. Hu, X.; Feng, G.; Duan, S.; Liu, L. A Memristive Multilayer Cellular Neural Network with Applications to Image Processing. *IEEE Trans. Neural Netw. Learn. Syst.* **2016**, *28*, 1889–1901. https://doi.org/10.1109/tnnls.2016.2552640.

73. Pham, V.-T.; Buscarino, A.; Fortuna, L.; Frasca, M. Autowaves in memristive cellular neural networks. *Int. J. Bifurc. Chaos* **2012**, *22*, 1230027. https://doi.org/10.1142/s0218127412300273.
74. Zidan, M.A.; Strachan, J.P.; Lu, W.D. The future of electronics based on memristive systems. *Nat. Electron.* **2018**, *1*, 22–29. https://doi.org/10.1038/s41928-017-0006-8.